



Early Eocene $^{40}\text{Ar}/^{39}\text{Ar}$ age for the Pampa de Jones plant, frog, and insect biota (Huitrera Formation, Neuquén Province, Patagonia, Argentina)

Peter WILF¹, Brad S. SINGER², María del Carmen ZAMALOA³, Kirk R. JOHNSON⁴ and N. Rubén CÚNEO⁵

Abstract. The Pampa de Jones fossil site, a stratigraphically isolated roadcut near the northeastern shore of Nahuel Huapi Lake in Neuquén Province, Argentina, holds a rich fossil biota including a macroflora, a microflora, insects, and most famously, an ontogenetic series of pipid frogs. The site exposes tuffaceous mudstone and sandstone beds of probable lacustrine origin, considered to belong to the volcanic Huitrera Formation. However, there have been no reliable age constraints for the fossil assemblage. We undertook laser fusion analyses of sanidine and biotite crystals occurring in a tuff layer found 4.4 m above the main fossil horizon. Twenty-eight sanidine crystals yielded an $^{40}\text{Ar}/^{39}\text{Ar}$ age of 54.24 ± 0.45 Ma that is preferred over our biotite age of 53.64 ± 0.35 Ma. Pampa de Jones is thus the oldest well-dated Eocene fossil site in Patagonia, predating two other recently $^{40}\text{Ar}/^{39}\text{Ar}$ -dated sites: Laguna del Hunco (51.91 ± 0.22 Ma) and Río Pichileufú (47.46 ± 0.05 Ma). The improved age control makes possible a finer scale of evolutionary hypothesis testing and turnover analysis in the region. The age is concordant with the site's placement in the Huitrera Formation and a depositional origin related to Early Paleogene arc volcanism, and it correlates to an interval of significant climate fluctuations following the Paleocene-Eocene boundary.

Resumen. EDAD $^{40}\text{Ar}/^{39}\text{Ar}$ PARA LA BIOTA DE PLANTAS, ANUROS E INSECTOS DEL EOCENO TEMPRANO DE PAMPA DE JONES (FORMACIÓN HUITRERA, PROVINCIA DEL NEUQUÉN, ARGENTINA). La localidad de Pampa de Jones es un afloramiento estratigráficamente aislado, cercano a la costa noreste del Lago Nahuel Huapi en la Provincia del Neuquén, Argentina. Contiene una rica biota fósil que incluye macroflora, microflora, insectos y una reconocida serie ontogenética de pípidos. La secuencia estratigráfica consiste de fangolitas y areniscas tufáceas de probable origen lacustre, asignada a la Formación Huitrera. La ausencia de datos geocronológicos directos ha impedido la estimación de edades confiables para esta paleobiota. En este trabajo se analizan por fusión láser los cristales de sanidina y biotita presentes en un nivel de toba ubicado a 4.4 m por encima del principal horizonte fosilífero. Veintiocho cristales de sanidina arrojaron una edad $^{40}\text{Ar}/^{39}\text{Ar}$ de 54.24 ± 0.45 Ma, la cual se prefiere a la edad de 53.64 ± 0.35 Ma estimada a partir de la biotita. La biota de Pampa de Jones es la más antigua del Eoceno de Patagonia datada radiométricamente, y precede a las dos localidades Eocenas datadas en la región: Laguna del Hunco (51.91 ± 0.22 Ma) y Río Pichileufú (47.46 ± 0.05 Ma). El control cronológico ajustado permitirá evaluar hipótesis evolutivas y analizar recambios en la región con una mayor resolución temporal. La edad obtenida concuerda con la ubicación de la secuencia dentro de la Formación Huitrera y con el origen de los depósitos asociados al volcanismo de arco del Paleógeno temprano, y se correlaciona con un lapso de significativas fluctuaciones climáticas ocurridas con posterioridad al pasaje Paleoceno-Eoceno.

Key words. Early Eocene. Huitrera Formation. Geochronology. Paleobotany. Patagonia. Neuquén. Argentina.

Palabras clave. Eoceno temprano. Formación Huitrera. Geocronología. Paleobotánica. Patagonia. Neuquén. Argentina.

Introduction

A significantly improved geochronologic framework for classic Eocene fossil deposits in Argentine Patagonia is emerging from paleomagnetic stratigraphy and analytically precise $^{40}\text{Ar}/^{39}\text{Ar}$ radioisotopic

dating (Kay *et al.*, 1999; Wilf *et al.*, 2003, 2005a; Gosses, 2006). The improved age control provides the necessary precision for diverse topics to be investigated, including clade dating, biogeographic patterns, and comparisons of climate change and biodiversity with disparate regions of South America and other continents (Petrulevičius and Nel, 2005; Wilf *et al.*, 2005b, 2009; Zamaloa *et al.*, 2006; Barreda and Palazzesi, 2007; Cione and Báez, 2007; Crisp *et al.*, 2009; Petrulevičius, 2009; Sarzetti *et al.*, 2009; Tejedor *et al.*, 2009).

The Pampa de Jones fossil locality of Neuquén Province, Patagonia, Argentina (also in the literature as "Nahuel Huapi" and "Nahuel Huapi Este"), contains an informative biota but is not reliably dated, limiting its usefulness in a broader evolutionary and stratigraphic framework. The site is an accessible but stratigraphically isolated roadcut outcrop of the

¹Department of Geosciences, Pennsylvania State University, University Park, Pennsylvania 16802, USA. pwilf@psu.edu

²Department of Geoscience, University of Wisconsin, Madison, Wisconsin 53706, USA. bsinger@geology.wisc.edu

³Facultad de Ciencias Exactas y Naturales, Universidad de Buenos Aires, Intendente Güiraldes 2620, 1428 Buenos Aires, Argentina. mzamaloa@ege.fcen.uba.ar

⁴Department of Earth Sciences, Denver Museum of Nature & Science, Denver, Colorado 80205, USA. KJohnson@dmns.org

⁵Museo Paleontológico Egidio Feruglio, CONICET, 9100 Trelew, Chubut, Argentina. rcuneo@mef.org.ar

Huitrera Formation within Nahuel Huapi National Park, exposed on both the north and south sides of Route 231 near the northeastern shore of Nahuel Huapi Lake, close to San Carlos de Bariloche (figures 1, 2). The local strata consist of tuff and mudstone, siltstone, and sandstone beds, somewhat more than 8 m thick on a single section line in the center of the outcrop (appendix 1), representing a volcanic lacustrine environment probably located near a lake margin (see also Aragón and Romero, 1984; Báez and Pugener, 2003; Melendi *et al.*, 2003). Most of the macrofossils at the site occur in a blocky, silty mudstone unit of 1 m thickness (appendix 1: Unit 16).

The best-known fossils from Pampa de Jones are a nearly complete ontogenetic sequence for the pipid frog *Llankibatrachus truebae* (Báez, 1996; Báez and Pugener, 2003) that is an important component of the rapidly emerging fossil history of Pipidae in Patagonia (Casamiquela, 1961; Báez and Trueb, 1997; Cione and Báez, 2007) and elsewhere (*e.g.*, Roček and Van Dijk, 2006; Rage and Dutheil, 2008). A palynoflora has also been described (Melendi *et al.*, 2003). Insects and plant macrofossils from the site are frequently mentioned in the literature (*e.g.*, Aragón and Romero, 1984) but have never been described or illustrated.

The outcrop lies within the mapped extent of Paleocene-Eocene volcanic arc rocks of the Pilcaniyeu Belt (equivalent to the Huitrera Formation of several authors), but its location is also near an Oligocene volcanic arc that generally crops out west of the Pilcaniyeu belt, known as the El Maitén belt (Rapela *et al.*, 1988). Cazau *et al.* (2005) most recently summarized the history of the highly inconsistent stratigraphic concepts used in this area (Feruglio, 1927; 1949; Rabassa, 1978; Ravazzoli and Sesana, 1977; González Bonorino and González Bonorino, 1978; González Bonorino, 1979; González Díaz, 1979; Rapela *et al.*, 1984, 1988; Cazau *et al.*, 1989; Mancini and Serna, 1989; Ardolino *et al.*, 2000). The entire framework would benefit from substantial revision incorporating new geochronologic data.

Within this setting, the age of the Pampa de Jones biota has remained unknown (Aragón and Romero, 1984; Báez and Pugener, 2003). The only relevant geochronologic data have been whole-rock K/Ar ages from locations with very uncertain correlations to the outcrop (González Díaz, 1979; Rapela *et al.*, 1983, 1984; Cazau *et al.*, 1989; Mazzoni *et al.*, 1991). Recently, Melendi *et al.* (2003) suggested an early Eocene age by correlating the palynological content of the outcrop. In particular, Melendi *et al.* relied on a stated early Eocene overlap of the known range endpoints of *Periporopollenites demarcatius* (Chenopodiaceae, Amaranthaceae, or Trimeniaceae) and *Plicatopollis wodehousei* (*cf.* Juglandaceae); the presence of triatriate pollen, including *P. wodehousei*, linked to Juglandaceae, Myricaceae, and Casuarinaceae, that Frederiksen and Chris-

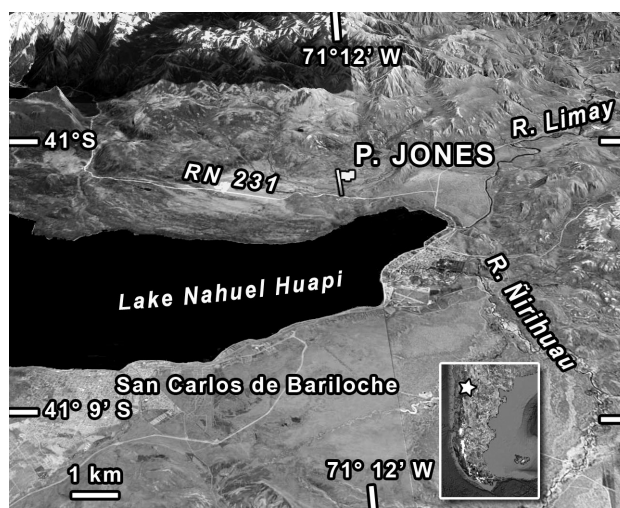


Figure 1. Location of the Pampa de Jones site (flag, "P. Jones") based from Google Earth (www.earth.google.com), using tilted three-dimensional view and 2x vertical exaggeration. Lake Nahuel Huapi and the Limay River together define the boundary between Río Negro (to south) and Neuquén (to north) provinces. Varying image contrast and a near-vertical line across the image are due to adjacent satellite coverage panels. Geographic coordinates for the site at our line of section are S41° 02' 20.0", W71° 12' 4.1" (WGS84 datum; appendix 1) / ubicación geográfica de Pampa de Jones (bandera, "P. Jones") basada en Google Earth (www.earth.google.com), usando vista tridimensional inclinada y exageración vertical de 2x. El Lago Nahuel Huapi y el Río Limay determinan el límite entre las provincias de Río Negro (al sur) y del Neuquén (al norte). Variaciones en el contraste de la imagen y una línea casi vertical atravesando la imagen se deben a coberturas satelitales adyacentes. Las coordenadas geográficas del sitio en nuestra línea de sección son S41° 02' 20.0", W71° 12' 4.1" (WGS84 datum; Apéndice 1).

topher (1978) found to decline markedly in middle Eocene to Oligocene assemblages from the southeastern USA; and the absence of *Nothofagidites* (pollen of *Nothofagus*). *Nothofagus* is widely considered to be absent in central and northern Patagonia during the warm early Eocene and to become abundant by the middle Eocene with climatic cooling (*e.g.*, Troncoso and Romero, 1998; Melendi *et al.*, 2003; Okuda *et al.*, 2006; Volkheimer and Narváez, 2006; Barreda and Palazzesi, 2007; Palazzesi and Barreda, 2007).

Although the early Eocene age for the Pampa de Jones biota that Melendi *et al.* (2003) proposed from palynological data is here confirmed, these data were not age diagnostic. *P. demarcatius* is only known in Argentina from imprecisely dated, probably middle Eocene rocks from Río Turbio, ~1200 km to the south of Pampa de Jones (Romero and Zamaloa, 1985; Malumián and Caramés, 1997), and otherwise from Australia, where it ranges from the early Eocene to the early Miocene in the Gippsland Basin (Stover and Partridge, 1973: p. 273). *P. wodehousei* is known in Argentina only from the early Paleocene Salamanca Formation at a site in Santa Cruz ~770 km south of Pampa de Jones (Zamaloa and Andreis, 1995), and Frederiksen and Christopher's (1978) data regarding

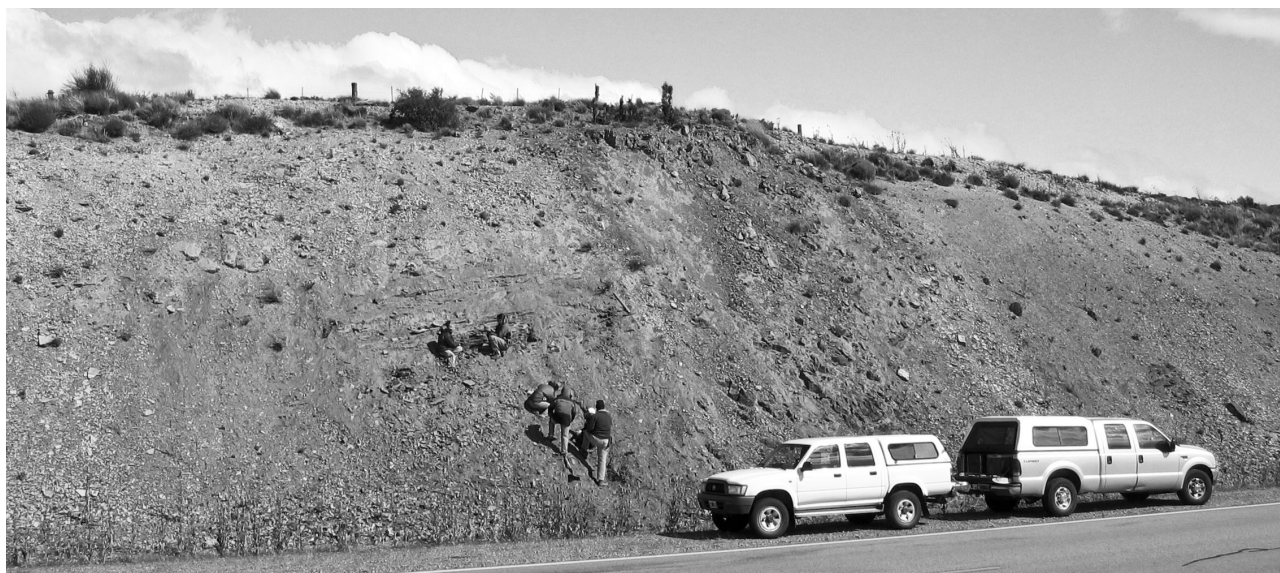


Figure 2. View of south (north-facing) side of the Pampa de Jones outcrop. Line of section (appendix 1) is being measured by the three workers at bottom. Principal fossil horizon is being excavated by the two workers above. The Pampa de Jones tuff is present at the top of the exposure and was sampled slightly to the east, where it was more freshly exposed at road level. Note dip to east, of 10° / *vista de la ladera sur (de cara al norte) del afloramiento de Pampa de Jones. La sección (Apéndice 1) está siendo medida por los tres investigadores al pie. Hacia arriba, el principal horizonte fosilífero está siendo excavado por otros 2 investigadores. La toba de Pampa de Jones se encuentra en el tope de la exposición y fue muestreada ligeramente hacia el este, donde presenta exposición más fresca a nivel de la ruta. Notar buzamiento hacia el este, de 10° .*

Plicatopollis came from a single core in South Carolina that did not contain *P. wodehousei*. The absence of *Nothofagus* from the early Eocene of Patagonia was described from a handful of floras, and none of these was reliably constrained to the early Eocene.

Interestingly, the nearby Confluencia locality (37 km to the north-northeast; Pascual and Odreman Rivas, 1973; Aragón and Romero, 1984), which has produced the only other occurrence of the pipid *Llankibatrachus truebae* (Báez *et al.*, 1990; Báez and Pugener, 2003), has a great abundance of *Nothofagus* pollen (Báez *et al.*, 1990; Melendi *et al.*, 2003). The only age control for Confluencia is very tentative, namely a whole-rock K-Ar date of 52 ± 3 Ma from a sampling location with uncertain relationship to the fossils (Rapela *et al.*, 1983, 1984).

We visited Pampa de Jones, sampled the thick tuff layer at the top of the exposure for $^{40}\text{Ar}/^{39}\text{Ar}$ analyses, and made preliminary fossil collections. Here, we report the results, discuss their regional and global implications, and provide a preliminary look at the macroflora.

Materials and methods

Our field work took place on 21 March, 2004 and 7 March, 2005. A single line of section was measured at the thickest exposure on the south (north-facing) side of the Pampa de Jones roadcut, where macrofossils are most accessible (figure 2; appendix 1). In order to refine stratigraphic understanding of the pollen content of the outcrop, pollen samples were collected from se-

veral horizons and processed using standard techniques; six horizons yielded palynomorphs as indicated in appendix 1. Approximately 100 plant macrofossils were collected using standard bench quarrying techniques, mostly consisting of angiosperm leaves but including some fruits and seeds as well as conifer material. These are under separate study, but because no plant macrofossils have been illustrated from Pampa de Jones since their existence was first mentioned in the literature (Aragón and Romero, 1984), we provide a sample here (figure 3), including some others from the site housed in the collections of the University of Buenos Aires (FCENCB-PB acronym). The number of species and preservational quality of specimens is not yet sufficient for paleoclimate analysis from leaf morphology (*e.g.*, Greenwood, 2007). The collection also includes several tadpoles of *Llankibatrachus truebae* and unidentified insects awaiting study. Specimens from the 2004 field trip are temporarily deposited at Administración de Parques Nacionales, Delegación Regional Patagonia, San Carlos de Bariloche (APN), awaiting a permanent repository assignment, and those from 2005 are deposited at the Museo Paleontológico Egidio Feruglio, Trelew (MPEF-Pb). The tuff sample was collected from the uppermost horizon in the measured section (appendix 1), after tracing down to road level along the 10°E dip for better access.

In the University of Wisconsin-Madison Rare Gas Geochronology Laboratory, sanidine and biotite separated from the tuff were cleaned, irradiated, and analyzed as single crystals, using a CO_2 laser to fuse the crystals and a fully automated gas-handling and

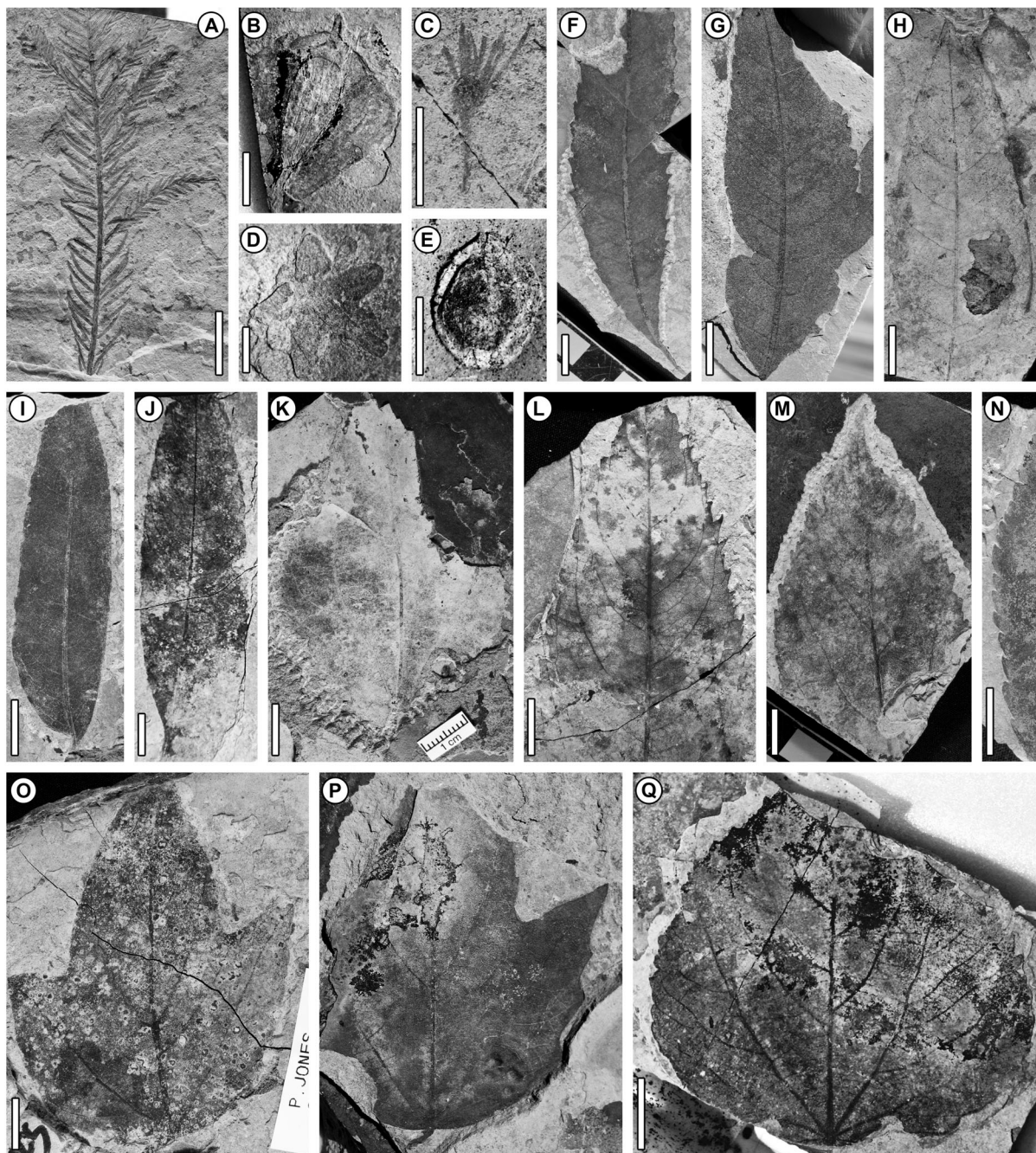


Figure 3. Preliminary sample of plant macrofossils from Pampa de Jones. Affinities unknown except where indicated. Additional descriptive details given in Appendix 3. Scale bars = 5 mm for B-E, 1 cm for others. Scale for (P) unavailable, but its size is similar to (O). If equivalent or similar to forms known from Laguna del Hunco (LH) or Río Pichileufú (RP), so indicated (Berry, 1938; Wilf et al., 2005a). / muestra preliminar de los macrofósiles vegetales de Pampa de Jones. Afinidades desconocidas, excepto cuando son indicadas. Detalles descriptivos adicionales se dan en Apéndice 3. Escala gráfica = 5 mm para B-E, 1 cm para el resto. Escala no disponible para (P), pero su tamaño es similar a (O). Si existen formas equivalentes o similares a las conocidas para Laguna del Hunco o Río Pichileufú, se indican (Berry, 1938; Wilf et al., 2005a). **A**, Podocarpaceae, foliage / Podocarpaceae, follaje, (LH, RP), APN. **B**, *Araucaria* cf. *A. pichileufensis* Berry, cone scale with seed / *Araucaria* cf. *A. pichileufensis* Berry, escama con semilla, (LH, RP), FCENCB-PB 270. **C**, angiosperm reproductive structure / estructura reproductiva de angiosperma, MPEF-Pb 3630. **D**, angiosperm flower / flor de angiosperma, FCENCB-PB 271. **E**, angiosperm seed / semilla de angiosperma, FCENCB-PB 272A. **F-G**, probable Cunoniaceae leaflets / probables folíolos de Cunoniaceae, (LH, RP), MPEF-Pb 3631 (F), APN (G). **H**, ovate, toothed angiosperm leaf morphotype / morfotipo foliar de angiosperma, ovado con márgen dentado, MPEF-Pb 3632. **I**, probable Fabaceae leaflet / probable folíolo de Fabaceae, MPEF-Pb 3633. **J**, elliptic angiosperm leaf morphotype / morfotipo foliar elíptico de angiosperma, FCENCB-PB 269A. **K-N**, angiosperm leaf morphotypes / morfotipos foliares de angiosperma, MPEF-Pb 3634 (K), MPEF-Pb 3635 (L), MPEF-Pb 3636 (M, ?Salicaceae), and MPEF-Pb 3637 (N). **O**, probable Malvaceae s.l. leaf morphotype / morfotipo foliar de probable Malvaceae s.l., MPEF-Pb 3638. **P**, second probable Malvaceae s.l. morphotype / segundo morfotipo foliar de probable Malvaceae s.l., APN. **Q**, angiosperm leaf morphotype similar to a form occurring at LH (morphotype TY057 of Wilf et al., 2005) / morfotipo foliar de angiosperma similar a uno registrado en LH (morfotipo TY057 de Wilf et al., 2005), FCENCB-PB 274A.

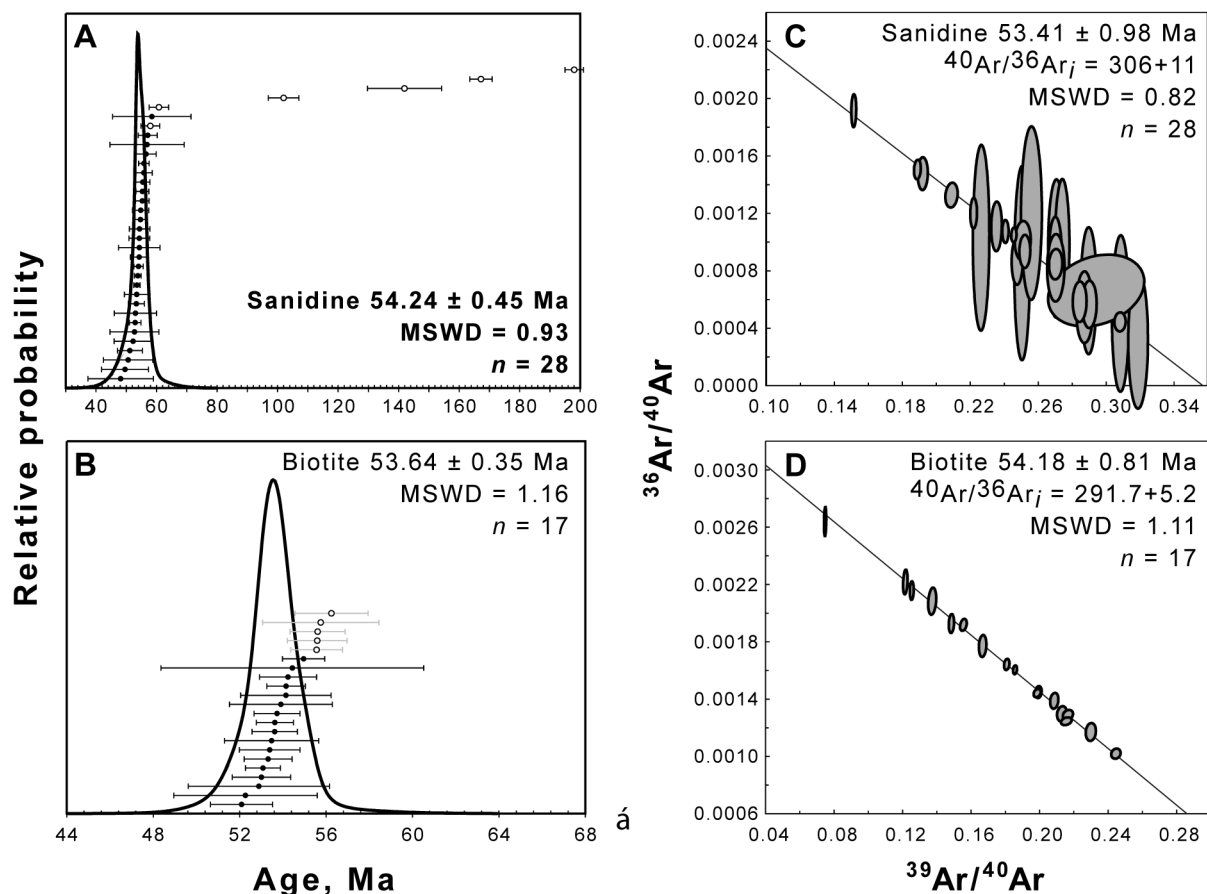


Figure 4. Apparent ages (A, B) and isochrons (C, D) calculated from the youngest sub-populations of measured sanidine (A, C) and biotite (B, D) crystals. Many older crystals (open symbols) plot off the diagrams and are not included in the weighted mean age or isochron calculations. The weighted mean of 28 sanidine crystals, 54.24 ± 0.45 Ma (A), is the preferred age of the Pampa de Jones tuff. All ages calculated relative to 28.34 Ma Taylor Creek rhyolite sanidine (equivalent to 28.02 Ma Fish Canyon Tuff sanidine). Uncertainties are $\pm 2\sigma$ / edades aparentes (A, B) e isócronas (C, D) calculadas a partir de las sub-poblaciones más jóvenes de cristales medidos de sanidina (A, C) y biotita (B, D). Muchos cristales más antiguos (símbolos abiertos) caen fuera de los diagramas y no fueron incluidos en la edad media ponderada ni en cálculos isocrónicos. La media ponderada de 28 cristales de sanidina, 54.24 ± 0.45 Ma (A), es la edad preferida para la toba de Pampa de Jones. Todas las edades fueron calculadas en relación a la sanidina de la riolita de Taylor Creek de 28.34 Ma (que es equivalente a la sanidina de la toba de Fish Canyon de 28.02 Ma). Las incertidumbres son de $\pm 2\sigma$.

mass-spectrometry system to measure the isotopic composition. Sample preparation, analytical methods and procedures for calculating $^{40}\text{Ar}/^{39}\text{Ar}$ ages are fully documented in Smith *et al.* (2008a). Uncertainties in age are reported at the 95% level of confidence ($\pm 2\sigma$).

Results

A total of 35 sanidine and 34 biotite crystals were fused and analyzed; apparent ages range from *ca.* 51 to 740 Ma for the sanidine and 52 to 617 Ma for the biotite

Table 1. Summary of $^{40}\text{Ar}/^{39}\text{Ar}$ laser-fusion experimental results, Pampa de Jones tuff / resumen de los resultados experimentales de fusión por láser $^{40}\text{Ar}/^{39}\text{Ar}$, toba de Pampa de Jones.

Experiment	n	Isochron Analysis			Average K/Ca $\pm 2\sigma$	Apparent age	
		MSWD	$^{40}\text{Ar}/^{36}\text{Ar}_i$	Age (Ma) $\pm 2\sigma$		MSWD	Age (Ma) $\pm 2\sigma$
Sanidine	28/35	0.82	306.0 ± 11.0	53.41 ± 0.98	0.30 ± 0.03	0.93	54.24 ± 0.45
Biotite	17/34	1.11	291.7 ± 5.2	54.18 ± 0.81	1.83 ± 0.70	1.16	53.64 ± 0.35
Combined		1.5	n/a	53.87 ± 0.62		4.40	53.87 ± 0.28

See appendix 2 for complete results. Bold indicates preferred age. All ages calculated relative to 28.34 Ma for the Taylor Creek rhyolite sanidine (Renne *et al.*, 1998) using the decay constants of Steiger and Jäger (1977). n = the number of experiments used to calculate the age versus the total number of experiments. MSWD = mean squared weighted deviate/ véase resultados completos en Apéndice 2. La negrita indica la edad preferida. Todas las edades fueron calculadas en relación a la sanidina de la riolita de Taylor Creek de 28.34 Ma (Renne *et al.*, 1998) usando las constantes de decaimiento de Steiger and Jäger (1977). n = número de experimentos usados para calcular la edad versus el número total de experimentos. MSWD = media cuadrática de desviaciones ponderadas.

(appendix 2). However, the youngest 28 sanidine and 17 biotite crystals yielded Gaussian probability distributions, strongly suggesting that crystals yielding older apparent ages are xenocrysts (figure 4). Excluding these older crystals, the inverse-variance weighted mean age of the 28 sanidine crystals is 54.24 ± 0.45 Ma; these define an inverse isochron age of 54.41 ± 0.98 Ma, with an atmospheric $^{40}\text{Ar}/^{36}\text{Ar}$ intercept value of 306 ± 11 . Likewise, 17 of the biotite crystals yielded an inverse-variance weighted mean age of 54.64 ± 0.35 Ma and an inverse isochron age of 54.18 ± 0.81 Ma, with an $^{40}\text{Ar}/^{36}\text{Ar}$ intercept value of 292 ± 5 (figure 4; table 1). The four ages are indistinguishable from one another, consistent with an eruption age of ca. 54 Ma. Because there is no evidence from the isochrons that excess argon is present in levels large enough to bias the age, and because biotite can be problematic owing to subtle alteration effects (Smith *et al.*, 2006, 2008b), we take the weighted mean age of 54.24 ± 0.45 Ma of the sanidine as the best estimate of time elapsed since deposition of the Pampa de Jones tuff.

The pollen samples yielded a composition that was, as expected, quite similar to that reported by Melendi *et al.* (2003) and was not studied in detail: a mixture of fungal spores and fruiting bodies, monolete and trilete spores from bryophytes and pteridophytes, bisaccate and trisaccate pollen of Podocarpaceae, and porate angiosperm pollen. There were no significant differences in palynological composition between sampling levels (appendix 1).

The macroflora so far studied (figure 3 and caption) shows some similarity to the ~2.3 m.y. younger Laguna del Hunco assemblages, though quantifying the overlap requires more data; the Laguna del Hunco floras are sampled approximately 60 times more heavily than Pampa de Jones (Wilf *et al.*, 2005a). However, the four most common leaf taxa at Laguna del Hunco are so far absent at Pampa de Jones, "*Celtis*" *ameghenoi*, "*Myrcia*" *chubutensis*, "*Tetracera*" *patagonica*, and "*Schmidelia*" *proedulis* (Wilf *et al.*, 2005a). In accord with the Pampa de Jones palynoflora, Podocarpaceae and *Araucaria* are present (figure 3.A, B), and there are no macrofossils comparable to *Nothofagus*.

Discussion

Our $^{40}\text{Ar}/^{40}\text{Ar}$ results place the formerly isolated Pampa de Jones site into a much broader framework, laying out several productive avenues for future research. The Pampa de Jones biota can now be compared in a reliable temporal context to other regional assemblages, particularly Laguna del Hunco and Río Pichileufú, to refine hypotheses about evolutionary dates, biotic turnover, and landscape and climate change. The age is consistent with deposition during AMEGHINIANA 47 (2), 2010

the Pilcaniyeu stage of volcanism (Rapela *et al.*, 1984); it provides a new, well-resolved constraint for interpreting regional magmatic history, though many more new ages are needed.

The Pampa de Jones assemblage is now the oldest Eocene macrofossil biota known in Patagonia (and probably in South America), providing a unique window into Patagonian ecosystems shortly after the Paleocene-Eocene boundary (55.8 Ma). Further investigation for paleoclimatic proxy data is merited to broaden understanding of significant climate fluctuations observed elsewhere near 54 Ma (Bao *et al.*, 1999; Wing *et al.*, 2000; Secord *et al.*, 2008; Zachos *et al.*, 2008; Chew, 2009). Pampa de Jones is now the only demonstrably early Eocene site in the region examined for *Nothofagus* pollen, supporting the idea that the genus was absent at this time (*e.g.*, Troncoso and Romero, 1998; Melendi *et al.*, 2003; Barreda and Palazzesi, 2007; Palazzesi and Barreda, 2007). However, we caution strongly against a broad regional and temporal interpretation using absence data from a single well-dated site. The nearby Confluencia locality has also produced the pipid *Llankibatrachus truebae*, but it has a different palynoflora from Pampa de Jones, including abundant *Nothofagus* pollen of both *brassii* and *fusca* types (Báez *et al.*, 1990; Melendi *et al.*, 2003). Accordingly, the Confluencia assemblages are considered middle Eocene or younger (Melendi *et al.*, 2003). Although a middle Eocene age is certainly possible, radioisotopic dating of the Confluencia deposits is needed to determine whether Confluencia is instead close in age to Pampa de Jones, which would indicate that the among-site difference in *Nothofagus* abundance is due to climate or landscape changes that are relatively closely spaced in time.

Acknowledgements

We thank the National Science Foundation, grants DEB-0345750 and DEB 0919071, for support of this research; A. Báez, an anonymous reviewer, and the Editor for helpful critiques; E. Aragón and A. Iglesias for critiquing earlier drafts; Parque Nacional Nahuel Huapi and C. Chehebar for site access; and R. Burnham, L. Canessa, B. Cariglino, M. Carvalho, E. Currano, C. González, P. Puerta, and E. Ruigomez for field and laboratory assistance.

References

- Aragón, E. and Romero, E.J. 1984. Geología, paleoambientes y paleobotánica de yacimientos Terciarios del occidente de Río Negro, Neuquén y Chubut. 9° Congreso Geológico Argentino (San Carlos de Bariloche), *Actas* 4: 475-507.
- Ardolino, A., M. Franchi, M. Remesal, and F. Salani. 2000. La sedimentación y el volcanismo terciarios en la Patagonia extraandina. 2. El volcanismo en la Patagonia extraandina. In: R. Caminos (ed.), *Geología Argentina. Servicio Geológico Minero Argentino, Instituto de Geología y Recursos Minerales, Anales* 29: 579-601.

- Báez, A.M. 1996. The fossil record of the Pipidae. In: R.C. Tinsley and H.R. Kobel (eds.), *The biology of Xenopus*. Symposia of the Zoological Society of London 68. Clarendon Press, Oxford, pp. 329-347.
- Báez, A.M. and Pugener, L.A. 2003. Ontogeny of a new Palaeogene pipid frog from southern South America and xenopodinomorph evolution. *Zoological Journal of the Linnean Society* 139: 439-476.
- Báez, A.M. and Trueb, L. 1997. Redescription of the Paleogene *Shelania pascuali* from Patagonia and its bearing on the relationships of fossil and Recent pipid frogs. *Scientific Papers, Natural History Museum, The University of Kansas* 4: 1-41.
- Báez, A.M., Zamaloa, M.C. and Romero, E.J. 1990. Nuevos hallazgos de microfloras y anuros Paleógenos en el Noroeste de Patagonia: implicancias paleoambientales y paleobiogeográficas. *Ameghiniana* 27: 83-94.
- Bao, H.M., Koch, P.L. and Rumble, D.I. 1999. Paleocene-Eocene climatic variation in western North America: evidence from the $\delta^{18}\text{O}$ of pedogenic hematite. *Geological Society of America Bulletin* 111: 1405-1415.
- Barreda, V. and Palazzesi, L. 2007. Patagonian vegetation turnovers during the Paleogene-early Neogene: origin of arid-adapted floras. *Botanical Review* 73: 31-50.
- Berry, E.W. 1938. Tertiary flora from the Río Pichileufú, Argentina. *Geological Society of America Special Paper* 12: 1-149.
- Casamiuela, R.M. 1961. Un pipoideo fósil de Patagonia. *Revista del Museo de La Plata, Sección Paleontología* 4: 71-123.
- Cazau, L., Mancini, D., Cangini, J. and Spalletti, L.A. 1989. Cuenca de Niriuhau. In: G.A. Chebli and L.A. Spalletti (eds.), *Cuencas sedimentarias Argentinas, Serie Correlación Geológica* no. 6. Universidad Nacional de Tucumán, Instituto Superior de Correlación Geológica, San Miguel de Tucumán, pp. 299-318.
- Cazau, L., Cortiñas, J., Reinante, S., Asensio, M., Bechis, F. and Aprenda, D. 2005. Cuenca de Niriuhau. In: G. Chebli, J.S. Cortiñas, L. Spalletti, L. Legarreta and E.L. Vallejo (eds.), *Frontera exploratoria de la Argentina. 6º Congreso de Exploración y Desarrollo de Hidrocarburos (Mar del Plata)*, *Actas* 1: 251-273.
- Chew, A.E. 2009. Paleocology of the early Eocene Willwood mammal fauna from the central Bighorn Basin, Wyoming. *Paleobiology* 35: 13-31.
- Cione, A.L. and Báez, A.M. 2007. Peces continentales y anfibios Cenozoicos de Argentina: los últimos cincuenta años. *Asociación Paleontológica Argentina. Publicación Especial* 11: 195-220.
- Crisp, M.D., Arroyo, M.T.K., Cook, L.G., Gandolfo, M.A., Jordan, G.J., McGlone, M.S., Weston, P.H., Westoby, M., Wilf, P. and Linder, H.P. 2009. Phylogenetic biome conservatism on a global scale. *Nature* 458: 754-756.
- Ellis, B., Daly, D., Hickey, L.J., Johnson, K.R., Mitchell, J., Wilf, P. and Wing, S.L. 2009. *Manual of leaf architecture*. Cornell University Press, Ithaca, 190 pp.
- Feruglio, E. 1927. Estudio geológico de la región pre- y subandina en la latitud del Nahuel Huapi. *Boletín de Informaciones Petroleras* 4: 425-434.
- Feruglio, E. 1949. *Descripción geológica de la Patagonia*, vol. II. Ministerio de Industria y Comercio de la Nación, Dirección General de Yacimientos Petrolíferos Fiscales, Buenos Aires, 349 pp.
- Frederiksen, N.O. and Christopher, R.A. 1978. Taxonomy and biostratigraphy of Late Cretaceous and Paleogene triartrate pollen from South Carolina. *Palynology* 2: 113-145.
- González Bonorino, F.G. 1979. Esquema de la evolución geológica de la Cordillera Norpatagónica. *Revista de la Asociación Geológica Argentina* 34: 184-202.
- González Bonorino, F.G. and González Bonorino, G.G. 1978. Geología de la región de San Carlos de Bariloche: un estudio de las formaciones Terciarias del Grupo Nahuel Huapi. *Revista de la Asociación Geológica Argentina* 33: 175-210.
- González Díaz, E.F. 1979. La edad de la Formación Ventana, en el área al norte y al este del Lago Nahuel Huapi. *Revista de la Asociación Geológica Argentina* 34: 113-124.
- Gosses, J. 2006. [Stratigraphy and $^{40}\text{Ar}/^{39}\text{Ar}$ geochronology of the Laguna del Hunco Formation: a lacustrine and sub-aerial caldera moat formation. Masters Thesis, Department of Geology and Geophysics, University of Wisconsin, Madison, Wisconsin, 265 pp. Unpublished.]
- Greenwood, D.R. 2007. Fossil angiosperm leaves and climate: from Wolfe and Dilcher to Burnham and Wilf. *Courier Forschungsinstitut Senckenberg* 258: 95-108.
- Kay, R.F., Madden, R.H., Vucetich, M.G., Carlini, A.A., Mazzoni, M.M., Re, G.H., Heizler, M. and Sandeman, H. 1999. Revised geochronology of the Casamayoran South American land mammal age: climatic and biotic implications. *Proceedings of the National Academy of Sciences USA* 96: 13235-13240.
- Malumíán, N. and Caramés, A. 1997. Upper Campanian-Paleogene from the Río Turbio coal measures in southern Argentina: micropaleontology and the Paleocene/Eocene boundary. *Journal of South American Earth Sciences* 10: 189-201.
- Mancini, C.D. and Serna, M.J. 1989. Evaluación petrolera de la Cuenca de Niriuhau, sudoeste de Argentina. *1º Congreso Nacional de Exploración de Hidrocarburos (Mar del Plata)*, *Actas* 2: 739-762.
- Mazzoni, M.M., Kawashita, K., Harrison, S. and Aragón, E. 1991. Edades radimétricas Eocenas. Borde occidental del Macizo Norpatagónico. *Revista de la Asociación Geológica Argentina* 46: 150-158.
- Melendi, D.L., Scafati, L.H. and Volkheimer, W. 2003. Palynostratigraphy of the Paleogene Huitrera Formation in N-W Patagonia, Argentina. *Neues Jahrbuch für Geologie und Paläontologie - Abhandlungen* 228: 205-273.
- Okuda, M., Nishida, H., Uemura, K. and Yabe, A. 2006. Paleocene/Eocene pollen assemblages from the Ligorio Márquez Formation, central Patagonia, XI Region, Chile. In: H. Nishida (ed.), *Post-Cretaceous floristic changes in southern Patagonia, Chile*. Faculty of Science and Engineering, Chuo University, Tokyo, pp. 37-43.
- Palazzesi, L. and Barreda, V. 2007. Major vegetation trends in the Tertiary of Patagonia (Argentina): a qualitative paleoclimatic approach based on palynological evidence. *Flora* 202: 328-337.
- Pascual, R. and Odreman Rivas, O. 1973. Las unidades estratigráficas del Terciario portadoras de mamíferos. Su distribución y sus relaciones con los acontecimientos diastróficos. *5º Congreso Geológico Argentino (Buenos Aires)*, *Actas* 3: 292-338.
- Petrulevičius, J.F. 2009. A panorpoid (Insecta: Mecoptera) from the lower Eocene of Patagonia, Argentina. *Journal of Paleontology* 83: 994-997.
- Petrulevičius, J.F. and Nel, A. 2005. Austroperilestidae, a new family of damselflies from early Eocene of Argentina (Insecta: Odonata). Phylogenetic relationships within Odonata. *Journal of Paleontology* 79: 658-662.
- Rabassa, J. 1978. Estratigrafía de la región de Pilcaniyeu. Comallo, Provincia de Río Negro. *7º Congreso Geológico Argentino (Neuquén)*, *Actas* 1: 731-746.
- Rage, J.C. and Dutheil, D.B. 2008. Amphibians and squamates from the Cretaceous (Cenomanian) of Morocco: a preliminary study, with description of a new genus of pipid frog. *Palaentographica Abteilung A* 285: 1-22.
- Rapela, C.W., Spalletti, L.A. and Merodio, J.C. 1983. Evolución magnética y geotectónica de la "Serie Andesítica" Andina (Paleoceno-Eoceno) en la Cordillera Norpatagónica. *Revista de la Asociación Geológica Argentina* 38: 469-484.
- Rapela, C.W., Spalletti, L.A., Merodio, J.C. and Aragón, E. 1984. El vulcanismo Paleoceno-Eoceno de la provincia volcánica Andino-Patagónica. *9º Congreso Geológico Argentino, Relatorio* 1: 189-213.
- Rapela, C.W., Spalletti, L.A., Merodio, J.C. and Aragón, E. 1988. Temporal evolution and spatial variation of early Tertiary volcanism in the Patagonian Andes (40° S-42°30' S). *Journal of South American Earth Sciences* 1: 75-88.
- Ravazzoli, I.A. and Sesana, F.L. 1977. Descripción geológica de la Hoja 41c, Río Chico, provincia de Río Negro. *Servicio Geológico Nacional (Buenos Aires)*, *Boletín* 148: 1-80.
- Renne, P.R., Swisher, C.C., Deino, A.L., Karner, D.B., Owens, T.L. and DePaolo, D.J. 1998. Intercalibration of standards, absolute ages and uncertainties in $^{40}\text{Ar}/^{39}\text{Ar}$ dating. *Chemical Geology* 145: 117-152.
- Roček, Z. and Van Dijk, E. 2006. Patterns of larval development in Cretaceous pipid frogs. *Acta Paleontologica Polonica* 51: 111-126.
- Romero, E.J. and Zamaloa, M.C. 1985. Polen de angiospermas de la Formación Río Turbio (Eoceno), Pcia. de Santa Cruz, Argentina. *Ameghiniana* 34: 207-214.
- Sarzetti, L.C., Labandeira, C.C., Muzón, J., Wilf, P., Cúneo, N.R., Johnson, K.R. and Genise, J.F. 2009. Odonatan endophytic oviposition from the Eocene of Patagonia: the ichnogenus *Paleoovoidus* and implications for behavioral stasis. *Journal of Paleontology* 83: 431-447.
- Secord, R., Wing, S.L. and Chew, A. 2008. Stable isotopes in early Eocene mammals as indicators of forest canopy structure and resource partitioning. *Paleobiology* 34: 282-300.
- Smith, M.E., Singer, B.S., Carroll, A.R. and Fournelle, J.H. 2006. High-resolution calibration of Eocene strata: $^{40}\text{Ar}/^{39}\text{Ar}$ geochronology of biotite in the Green River Formation. *Geology* 34: 393-396.
- Smith, M.E., Carroll, A.R. and Singer, B.S. 2008a. Synoptic reconstruction of a major ancient lake system: Eocene Green River Formation, western United States. *Geological Society of America Bulletin* 120: 54-84.
- Smith, M.E., Singer, B.S., Carroll, A.R. and Fournelle, J.H. 2008b. Precise dating of biotite in distal volcanic ash: isolating subtle alteration using $^{40}\text{Ar}/^{39}\text{Ar}$ laser incremental heating and electron microprobe techniques. *American Mineralogist* 93: 784-795.
- Steiger, R.H. and Jäger, E. 1977. Subcommittee on geochronology: convention on the use of decay constants in geo- and cosmochronology. *Earth and Planetary Science Letters* 36: 359-362.
- Stover, L.E. and Partridge, A.D. 1973. Tertiary and Late Cretaceous spores and pollen from the Gippsland Basin,

- southeastern Australia. *Proceedings of the Royal Society of Victoria* 85: 237-286.
- Tejedor, M.F., Goin, F.J., Gelfo, J.N., López, G., Bond, M., Carlini, A.A., Scillato-Yané, G.J., Woodburne, M.O., Chornogubsky, L., Aragón, E., Reguero, M.A., Czaplewski, N.J., Vincon, S., Martin, G.M. and Ciancio, M.R. 2009. New early Eocene mammalian fauna from western Patagonia, Argentina. *American Museum Novitates* 3638: 1-43.
- Troncoso, A. and Romero, E.J. 1998. Evolución de las comunidades florísticas en el extremo sur de Sudamérica durante el Cenofítico. *Monographs in Systematic Botany from the Missouri Botanical Garden* 68: 149-172.
- Volkheimer, W. and Narváez, P. 2006. Nuevos hallazgos de palinofloras del Paleógeno en el Norte Patagónico (Argentina). Significado estratigráfico, paleoclimático y paleoambiental. *13° Simposio Argentino de Paleobotánica y Palinología (Bahía Blanca), Resúmenes*: 82.
- Wilf, P., Cúneo, N.R., Johnson, K.R., Hicks, J.F., Wing, S.L. and Obradovich, J.D. 2003. High plant diversity in Eocene South America: evidence from Patagonia. *Science* 300: 122-125.
- Wilf, P., Johnson, K.R., Cúneo, N.R., Smith, M.E., Singer, B.S. and Gandolfo, M.A. 2005a. Eocene plant diversity at Laguna del Hunco and Río Pichileufú, Patagonia, Argentina. *American Naturalist* 165: 634-650.
- Wilf, P., Labandeira, C.C., Johnson, K.R. and Cúneo, N.R. 2005b. Richness of plant-insect associations in Eocene Patagonia: a legacy for South American biodiversity. *Proceedings of the National Academy of Sciences USA* 102: 8944-8948.
- Wilf, P., Little, S.A., Iglesias, A., Zamalao, M.C., Gandolfo, M.A., Cúneo, N.R. and Johnson, K.R. 2009. *Papuacedrus* (Cupressaceae) in Eocene Patagonia, a new fossil link to Australasian rainforests. *American Journal of Botany* 96: 2031-2047.
- Wing, S.L., Bao, H. and Koch, P.L. 2000. An early Eocene cool period? Evidence for continental cooling during the warmest part of the Cenozoic. In: B.T. Huber, K. MacLeod and S.L. Wing (eds.), *Warm climates in Earth history*. Cambridge University Press, Cambridge, pp. 197-237.
- Zachos, J.C., Dickens, G.R. and Zeebe, R.E. 2008. An early Cenozoic perspective on greenhouse warming and carbon-cycle dynamics. *Nature* 451: 279-283.
- Zamalao, M.C. and Andreis, R.R. 1995. Asociación palinológica del Paleoceno temprano (Formación Salamanca) en Ea. Laguna Manantiales, Santa Cruz, Argentina. *6° Congreso Argentino de Paleontología y Bioestratigrafía (Trelew), Actas*: 301-305.
- Zamalao, M.C., Gandolfo, M.A., González, C.C., Romero, E.J., Cúneo, N.R. and Wilf, P. 2006. Casuarinaceae from the Eocene of Patagonia, Argentina. *International Journal of Plant Sciences* 167: 1279-1289.

Recibido: 20 de mayo de 2009.

Aceptado: 20 de octubre de 2009.

Appendix 1. Measured stratigraphic section at Pampa de Jones* / sección estratigráfica medida en Pampa de Jones*

Unit#	Thickness, cm	Total thickness, cm	Lithology and notes
19		270+	Green tuff. Sampled where it comes down to the road, at about 140 cm.
18	225	730	Zone of interbedded medium-gray to light-gray mudstone, becomes buried and clastic at 70 cm.
17	74	505	Coarse yellow sandstone.
16	100	431	Blocky, laminated silty mudstone with fossil plants (mostly leaves), insects, and frogs. The main macrofossil layer.
15	3	331	Medium-gray mudstone.
14	15	328	Massive light-gray siltstone, very hard.
13	19	313	Medium gray silty claystone.
12	29	294	Yellow rusty fine-grained to very fine-grained sandstone.
11	19	265	Massive silty mudstone.
10	35	246	Brown-yellow to gray laminated, very fine-grained silty mudstone to claystone paper shale. Palynomorphs present.
9	19	211	Brownish-yellowish silty mudstone, well bedded. Palynomorphs present.
8	13	192	Medium gray silty mudstone. Palynomorphs present.
7	16	179	Mustard-colored, very fine-grained sandstone with thin organic layer at 10-12 cm.
6	35	163	Greenish-gray silty claystone. Palynomorphs present.
5	13	128	Rusty, fine-grained sandstone.
4	83	115	Well bedded-laminated gray mudstone, brown in middle and becoming gray at top. Palynomorphs present.
3	14	32	Yellowish brown, fine-grained sandstone.
2	18	18	Greenish gray silty mudstone. Palynomorphs present.
1			Fine-medium grained sandstone, blue with rusty joints.

*From road level to top of hill on southern (north-facing) exposure of roadcut, at center of outcrop. Strike 0° (no adjustment). Dip 10°E/ *desde el nivel de la ruta hasta el tope de la elevación, sobre la ladera sur (de cara al norte), en el centro del afloramiento. Rumbo 0° (sin ajuste). Buzamiento 10°E.

Appendix 2. Complete $^{40}\text{Ar}/^{39}\text{Ar}$ single step single crystal fusion results, Pampa de Jones tuff / *resultados completos de la fusión $^{40}\text{Ar}/^{39}\text{Ar}$ por láser realizada en un único cristal en un solo paso, toba de Pampa de Jones.*

Experiment	Laser Power (W)	$^{40}\text{Ar}/^{39}\text{Ar} \pm 2\sigma$	$^{237}\text{Ar}/^{39}\text{Ar} \pm 2\sigma$	$^{36}\text{Ar}/^{39}\text{Ar} \pm 2\sigma$	$^{40}\text{Ar} \times 10^{-14}$ mol	$^{40}\text{Ar}^*$	% K/Ca	Apparent age $\pm 2\sigma$ Ma
Sanidine			$J = 0.010728 \pm 0.3\%$	$\mu = 1.0069 \pm 0.03\% \ 1\sigma$				
BC6323	10.5	6.571 ± 0.048	0.71735 ± 0.01209	0.01279 ± 0.00061	0.83876	43.32	0.599	54.30 ± 3.45
BC6324	10.5	5.283 ± 0.043	0.75454 ± 0.01384	0.00817 ± 0.00029	1.08421	55.41	0.570	55.82 ± 1.72
BC6325	10.5	4.072 ± 0.023	1.08631 ± 0.01720	0.00457 ± 0.00017	1.13813	68.89	0.396	53.53 ± 1.02
BC6331	10.5	4.040 ± 0.042	0.70265 ± 0.01421	0.00372 ± 0.00055	0.23358	74.14	0.612	57.09 ± 3.14
BC6332	10.5	4.245 ± 0.047	1.62519 ± 0.02894	0.00515 ± 0.00060	0.34555	67.14	0.264	54.40 ± 3.40
BC6333*	10.5	5.438 ± 0.099	1.11786 ± 0.02917	0.00790 ± 0.00052	0.42533	58.69	0.384	60.78 ± 3.22
BC6335*	10.5	4.084 ± 0.064	1.69242 ± 0.03576	0.00398 ± 0.00053	0.44698	74.41	0.254	57.94 ± 3.10
BC6336	10.5	3.969 ± 0.042	1.22613 ± 0.02374	0.00405 ± 0.00038	0.62913	72.24	0.350	54.69 ± 2.18
BC6337	10.5	3.485 ± 0.046	1.13958 ± 0.02232	0.00206 ± 0.00058	0.33616	85.05	0.377	56.52 ± 3.34
BC6339	10.5	3.520 ± 0.040	1.37113 ± 0.02872	0.00243 ± 0.00041	0.51145	82.58	0.313	55.44 ± 2.36
BC6340	10.5	3.700 ± 0.043	2.13567 ± 0.04534	0.00371 ± 0.00032	0.39322	74.88	0.201	52.92 ± 1.93
BC6341	10.5	3.985 ± 0.060	1.29344 ± 0.03257	0.00437 ± 0.00045	0.50793	70.07	0.332	53.30 ± 2.65
BC6343	10.5	4.501 ± 0.033	1.32406 ± 0.02231	0.00577 ± 0.00039	0.79820	64.39	0.324	55.28 ± 2.24
BC6344	10.5	4.778 ± 0.070	1.61527 ± 0.03557	0.00678 ± 0.00034	0.46551	60.69	0.266	55.33 ± 2.15
BC6345	10.5	4.154 ± 0.026	1.30751 ± 0.02312	0.00482 ± 0.00027	0.88400	68.17	0.329	54.04 ± 1.56
BC6347	10.5	5.197 ± 0.065	1.19344 ± 0.02705	0.00800 ± 0.00049	0.74102	56.27	0.360	55.78 ± 2.81
BC6348	10.5	3.250 ± 0.028	1.36257 ± 0.02585	0.00181 ± 0.00018	0.67090	86.75	0.315	53.81 ± 1.09
BC6349	10.5	3.705 ± 0.041	1.24418 ± 0.02538	0.00379 ± 0.00074	0.25884	72.34	0.345	51.19 ± 4.15
BC6351	10.5	3.487 ± 0.042	1.78402 ± 0.03515	0.00265 ± 0.00050	0.25336	81.50	0.241	54.25 ± 2.86
BC6352	10.5	3.451 ± 0.041	1.43052 ± 0.02628	0.00234 ± 0.00046	0.37068	83.14	0.300	54.75 ± 2.67
BC7411*	10.5	16.953 ± 0.504	1.33535 ± 0.04604	0.03192 ± 0.00183	1.07912	44.97	0.322	141.94 ± 12.24
BC7412*	10.5	6.519 ± 0.253	1.40281 ± 0.04967	0.00410 ± 0.00040	0.68363	83.08	0.306	101.98 ± 5.05
BC7413*	10.5	30.481 ± 0.208	1.30253 ± 0.03215	0.07288 ± 0.00068	7.05868	29.68	0.330	167.23 ± 3.68
BC7415*	10.5	12.860 ± 0.159	1.71044 ± 0.04176	0.00741 ± 0.00028	2.30551	84.01	0.251	198.05 ± 3.08
BC7416*	10.5	50.277 ± 0.329	0.73189 ± 0.01856	0.01044 ± 0.00068	5.44292	93.98	0.587	740.06 ± 4.86
BC7417	10.5	3.405 ± 0.266	1.20612 ± 0.03919	0.00258 ± 0.00067	0.32804	80.32	0.356	52.22 ± 6.24
BC7419	10.5	3.652 ± 0.047	1.71690 ± 0.04494	0.00403 ± 0.00138	0.20242	71.06	0.250	49.59 ± 7.75
BC7420	10.5	3.699 ± 0.053	1.07223 ± 0.03372	0.00383 ± 0.00145	0.14537	71.67	0.401	50.63 ± 8.14
BC7421	10.5	3.456 ± 0.045	1.27429 ± 0.03297	0.00263 ± 0.00125	0.17998	80.34	0.337	53.01 ± 6.97
BC7423	10.5	3.142 ± 0.046	1.92966 ± 0.05488	0.00151 ± 0.00122	0.16605	90.52	0.223	54.29 ± 6.85
BC7424	10.5	3.993 ± 0.059	1.58617 ± 0.04673	0.00384 ± 0.00220	0.11303	74.70	0.271	56.88 ± 12.25
BC7425	10.5	3.907 ± 0.075	2.19080 ± 0.06663	0.00528 ± 0.00193	0.09647	64.43	0.196	48.14 ± 10.82
BC7427	10.5	4.412 ± 0.076	1.99522 ± 0.06059	0.00508 ± 0.00233	0.10224	69.47	0.215	58.44 ± 12.96
BC7428	10.5	3.248 ± 0.044	1.07541 ± 0.03858	0.00193 ± 0.00145	0.15450	85.02	0.400	52.71 ± 8.08
BC7429	10.5	3.701 ± 0.056	1.74370 ± 0.04745	0.00351 ± 0.00071	0.31269	75.63	0.246	53.44 ± 4.06
Inverse isochron age $\pm 2\sigma$ 53.41 ± 0.98			weighted plateau	n	28/35.Total fusions age $\pm 2\sigma$			94.26 ± 0.83
$^{40}\text{Ar}/^{39}\text{Ar}$ intercept $\pm 2\sigma$ $.306.0 \pm 11.0$				MSWD	0.93.Weighted mean age $\pm 2\sigma$			54.24 ± 0.45
Biotite			$J = 0.010572 \pm 0.2\% \ \mu = 1.0069 \pm 0.03\% \ 1\sigma$					
BC7046	10.5	5.532 ± 0.039	0.13457 ± 0.00307	0.00915 ± 0.00018	4.41199	51.28	3.195	53.32 ± 1.11
BC7047*	10.5	5.837 ± 0.068	0.05430 ± 0.00151	0.00963 ± 0.00026	1.74120	51.32	7.919	56.25 ± 1.69
BC7049	10.5	5.389 ± 0.027	0.06091 ± 0.00185	0.00869 ± 0.00013	1.99596	52.41	7.059	53.08 ± 0.81
BC7050	10.5	4.626 ± 0.052	0.05258 ± 0.00137	0.00601 ± 0.00014	3.37689	61.68	8.177	53.62 ± 1.05
BC7051	10.5	5.017 ± 0.037	0.22757 ± 0.00498	0.00736 ± 0.00017	6.04885	56.99	1.889	53.73 ± 1.06
BC7055	10.5	13.207 ± 0.101	0.16432 ± 0.00457	0.03493 ± 0.00109	1.70801	21.94	2.617	54.44 ± 6.08
BC7056*	10.5	5.754 ± 0.057	0.18236 ± 0.00430	0.00951 ± 0.00018	2.73818	51.40	2.358	55.56 ± 1.20
BC7057	10.5	6.425 ± 0.068	0.06780 ± 0.00191	0.01238 ± 0.00022	3.78442	43.12	6.342	52.09 ± 1.44
BC7059*	10.5	5.276 ± 0.058	0.23274 ± 0.00529	0.00789 ± 0.00018	2.03790	56.12	1.847	55.61 ± 1.27
BC7060*	10.5	4.709 ± 0.055	0.11562 ± 0.00311	0.00594 ± 0.00020	2.08414	62.86	3.719	55.59 ± 1.38
BC7061*	10.5	6.048 ± 0.049	0.13180 ± 0.00298	0.00631 ± 0.00021	5.44382	69.32	3.262	78.25 ± 1.33
BC7062*	10.5	5.054 ± 0.046	0.04943 ± 0.00136	0.00308 ± 0.00005	4.63067	82.03	8.699	77.39 ± 0.80

Appendix 2. (Continuation / *continuación*)

BC7064	10.5	6.716 ± 0.060	0.47117 ± 0.01064	0.01310 ± 0.00036	3.68717	42.89	0.912	54.14 ± 2.09
BC7065*	10.5	8.156 ± 0.072	0.15515 ± 0.00386	0.01759 ± 0.00048	3.94635	36.40	2.771	55.75 ± 2.69
BC7400*	10.5	22.117 ± 0.172	0.18839 ± 0.00521	0.02466 ± 0.00020	9.70330	67.11	2.282	263.00 ± 2.45
BC7402*	10.5	21.074 ± 0.184	0.09096 ± 0.00270	0.00802 ± 0.00020	19.52683	88.78	4.727	325.62 ± 2.88
BC7404*	10.5	41.337 ± 0.206	0.07233 ± 0.00270	0.00943 ± 0.00021	8.95014	93.27	5.944	616.82 ± 2.84
BC7405*	10.5	14.026 ± 0.063	0.12919 ± 0.00328	0.00542 ± 0.00016	13.92362	88.64	3.328	222.79 ± 1.26
BC7407*	10.5	13.587 ± 0.107	0.05796 ± 0.00197	0.01793 ± 0.00027	5.04527	61.02	7.418	151.60 ± 1.99
BC7408*	10.5	16.489 ± 0.077	0.05558 ± 0.00147	0.01890 ± 0.00024	12.52654	66.15	7.736	196.90 ± 1.61
BC7409	10.5	7.264 ± 0.105	0.15975 ± 0.00433	0.01521 ± 0.00056	2.04048	38.28	2.691	52.27 ± 3.32
BC7459*	10.5	29.514 ± 0.164	0.08709 ± 0.00244	0.01052 ± 0.00028	21.65685	89.49	4.937	444.27 ± 2.66
BC7460*	10.5	14.954 ± 0.092	0.06570 ± 0.00187	0.01361 ± 0.00021	8.19568	73.14	6.545	197.42 ± 1.64
BC7461*	10.5	14.857 ± 0.131	0.18058 ± 0.00467	0.02676 ± 0.00050	7.36521	46.87	2.381	128.17 ± 3.02
BC7463*	10.5	21.380 ± 0.161	0.12584 ± 0.00342	0.01318 ± 0.00044	7.30787	81.83	3.417	306.19 ± 3.17
BC7464	10.5	4.645 ± 0.057	0.11127 ± 0.00304	0.00584 ± 0.00011	2.75832	62.99	3.864	54.96 ± 0.98
BC7465	10.5	7.947 ± 0.058	0.23897 ± 0.00655	0.01725 ± 0.00043	2.90916	36.10	1.799	53.91 ± 2.38
BC7467	10.5	8.197 ± 0.074	0.16503 ± 0.00484	0.01826 ± 0.00057	2.58268	34.33	2.605	52.89 ± 3.27
BC7468	10.5	4.098 ± 0.038	0.03555 ± 0.00116	0.00422 ± 0.00012	2.37572	69.64	12.095	53.63 ± 0.86
BC7469	10.5	5.991 ± 0.062	0.10309 ± 0.00292	0.01067 ± 0.00037	2.34401	47.50	4.171	53.48 ± 2.18
BC7471	10.5	4.699 ± 0.051	0.11612 ± 0.00334	0.00616 ± 0.00020	3.07011	61.43	3.703	54.24 ± 1.32
BC7472	10.5	5.039 ± 0.043	0.10919 ± 0.00322	0.00733 ± 0.00012	1.72440	57.19	3.938	54.15 ± 0.89
BC7473	10.5	4.358 ± 0.048	0.11490 ± 0.00323	0.00516 ± 0.00022	1.62770	65.20	3.742	53.39 ± 1.40
BC7474	10.5	4.801 ± 0.046	0.06152 ± 0.00166	0.00672 ± 0.00021	2.91524	58.74	6.990	53.01 ± 1.35
Inverse isochron age ± 2σ	54.18 ± 0.81		weighted plateau	n	17/34	Total fusions age ± 2σ		128.39 ± 0.60
⁴⁰ Ar/ ³⁹ Ar intercept ± 2σ	291.7 ± 5.2			MSWD	1.16	Weighted mean age ± 2σ		53.64 ± 0.48

All ages calculated relative to 28.34 Ma for the Taylor Creek rhyolite sanidine (Renne *et al.*, 1998) using the decay constants of Steiger and Jäger (1977). Uncertainties in Ar isotope ratios and ages reported at 2σ analytical precision. All ages corrected for ³⁷Ar and ³⁹Ar decay, half lives of 35.2 days and 269 years, respectively / *todas las edades fueron calculadas en relación a la sanidina de la riolita de Taylor Creek de 28.34 Ma (Renne et al., 1998) usando las constantes de decaimiento de Steiger y Jäger (1977). Las incertidumbres en las proporciones de los isótopos de Ar y en las edades se indican con precisión analítica de 2σ. Todas las edades fueron corregidas por el decaimiento del ³⁷Ar y del ³⁹Ar, con vidas medias de 35.2 días y 269 años, respectivamente.*

*Analyses or experiments excluded from the weighted mean age calculation / *análisis o experimentos excluidos del cálculo de la edad media ponderada.*

Appendix 3. Additional description of selected fossils shown in Figure 3/ *descripción adicional de los fósiles seleccionados mostrados en la figura 3.*

Descriptive terminology for distinctive features from Ellis *et al.* (2009) / *para los rasgos distintivos se aplica la terminología descriptiva de Ellis et al. (2009).* **F-G**, equivalent to “*Cupania*” latifolioides Berry (1938: *sensu* plate 30, figure 1)/ *equivalente a “Cupania” latifolioides Berry (1938: según lámina 30, figura 1).* **I**, leaflet, asymmetrical, with untoothed margin and numerous, thin, brochidodromous secondary veins. Pulvinulus not preserved. Similar foliage is common at both Laguna del Hunco and Río Pichileufú (e.g., “*Cassia*” argentinensis Berry)/ *foliolo, asimétrico, con margen entero y numerosas venas secundarias delgadas y broquidódromas. Pulvínulos no preservados. Follaje similar es común tanto en Laguna del Hunco como en Río Pichileufú (p.e., “Cassia” argentinensis Berry).* **J**, numerous secondary and intersecondary veins, untoothed margin / *numerosas venas secundarias e intersecundarias, margen entero.* **K**, actinodromous primary venation, agrophic veins, opposite percurrent tertiary veins oriented perpendicular to primaries, and bluntly toothed margin/ *venación primaria actinódroma, venas agróficas, venas terciarias opuestas percurrentes orientadas perpendicularmente a las primarias y margen con dientes romos.* **L**, leaf distal portion with strong intersecondaries, well-preserved high-order venation, and large, narrow, irregular teeth with concave apical flanks and variable basal flanks / *porción distal de hoja con venas intersecundarias ro-*

bustas, venación de alto orden bien preservada y dientes grandes, angostos, irregulares, con lado apical cóncavo y lado basal variable. **M**, distal leaf portion having closely spaced, blunt, teeth with conspicuous apical glands/ *porción distal de hoja con dientes poco espaciados, romos, con conspicuas glándulas apicales.* **N**, leaf margin (remainder of leaf poorly preserved) showing distinctive teeth that are irregularly sized, large, closely spaced, and deeply incised with convex proximal flanks/ *margen de hoja (reminiscente a una hoja pobremente preservada) mostrando dientes característicos grandes, de tamaño irregular, poco espaciados y profundamente incisos con lados proximales convexos.* **O**, rounded base, three convex-sided lobes, rounded lobe sinuses, three stout, actinodromous primary veins, agrophic veins, and untoothed margin. A similar form is found at Laguna del Hunco (e.g., Wilf *et al.*, 2003: fig. 1.J) / *base redondeada, tres lóbulos de lados convexos y senos redondeados, tres venas primarias robustas, actinódromas, venas agróficas, y margen entero. Una forma similar se encuentra en Laguna del Hunco (p.e., Wilf et al., 2003: fig. 1.J).* **P**, similar to previous but with a toothed margin, preserving orthogonal reticulate high-order venation/ *similar a la anterior pero con margen dentado, venación de alto orden reticulada ortogonal preservada.* **Q**, seven actinodromous primary veins, compound agrophic veins with conspicuously forking minor secondaries, concentric percurrent tertiary veins, and toothed margin/ *siete venas primarias actinódromas, venas agróficas compuestas con secundarias menores conspicuamente bifurcadas, venas terciarias percurrentes concéntricas y margen dentado.*